



Experimental Behaviour of Friction-Based EradiQuake Seismic Isolation Systems

H. Fatemi¹, J. Conklin²

¹ Research and development engineer, Canam Bridges Canada Inc., Laval, QC, Canada.

² Engineering manager, RJ Watson Inc., Alden, NY, USA.

ABSTRACT

Nowadays, bridge owners are showing more interest in seismically isolated bridges in regions with considerable risk of seismicity. The reason is rooted in the facts that: i) seismically isolated bridges have performed satisfyingly in recent seismic events. Records from these structures show good correlation between the analytical prediction and the field performance; and ii) the seismic isolation offers a more economical alternative in the bridge construction industry by using much less materials in the structural elements of isolated bridges. Different seismic isolation systems are available to use in bridges, but fewer test results showing the experimental behaviour of these elements, in full-scale, are available. Two full-scale friction-based EradiQuake isolators subjected to both qualification and quality tests, were tested in this program. These isolators, designed and fabricated as the seismic isolation system of a bridge in Canada, were tested mainly in the structural laboratory at Ecole Polytechnique de Montréal. In this paper, the results of full-scale tests, carried out as per CAN CSA S6 and project specifications, both at the room and cold temperatures, are presented and the experimental behaviour of EradiQuake isolators is discussed. Results showed that the EradiQuake system has great flexibility to adjust to the project needs. The tested seismic isolation systems displayed a very good capacity of energy dissipation and showed an effective stiffness in the target range in both ambient and low temperature tests. The paper provides some recommendations to improve the test methods addressed in the Canadian and American standards. These test results could provide a deeper insight, for bridge engineers and researchers, into the ambient and cold temperature behaviour of EradiQuake isolation systems that affect the performance of bridges. The isolators were recently installed on the bridge and currently are in service.

Keywords: seismic isolation, EradiQuake, effective stiffness, energy dissipation.

INTRODUCTION

Seismic events could severely damage critical infrastructures including bridges. This threat has led to the need to design and construct seismically resistant highway bridges and viaducts. Seismic isolation reduces shear forces by shifting the fundamental period of the structure. Figure 1a shows the effect of seismic isolation on the design spectrum of a typical bridge. Period elongation will shift the structure in the spectrum sensitivity zone and change the damping effect. According to Datta [1], a spectrum can be divided into three zones: i) a displacement sensitive zone (long period region); ii) an acceleration sensitive zone (short period region); and iii) a velocity sensitive region (intermediate period region). By shifting the period from one zone to another zone the effect of damping and force demands during a seismic event will be changed. The isolated structure possesses an elongated fundamental period that shifts the structure from the acceleration sensitive zone to the velocity or displacement sensitive zones.

A wide variety of seismic isolation systems are being used in bridges and other structures, but fewer test results showing the experimental behaviour of these elements, in full-scale, are available. Results of the tests as per the standards in practise could provide a deeper insight, for engineers and researchers, into the dynamic behaviour of isolation systems that affect the performance of structures.

A theoretical force-displacement hysteresis loop of a seismic isolator is presented in Figure 1b. In this figure, Q_d represents the characteristic strength of the isolator, F_y denotes the yield strength, F_{max} shows the maximum force corresponding to the design displacement, K_d stands for the post elastic stiffness, K_u is the elastic stiffness, K_{eff} shows the effective stiffness of the isolator, Δ_{max} is the design displacement, and EDC denotes dissipated energy per each hysteresis loop.

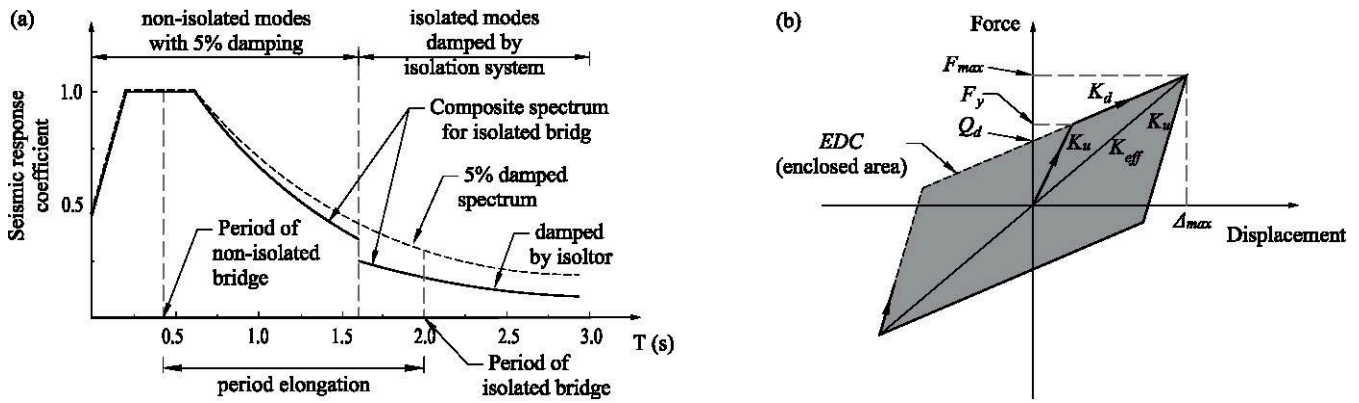


Figure 1. (a): Typical design response spectrum for an isolated bridge, adopted from AASHTO GSFSID [2]; (b): Characteristics of bilinear isolation bearings.

FRICITION-BASED ISOLATION SYSTEMS

In friction-based isolation systems, the imposed seismic energy is mainly dissipated through a friction surface that is generally polytetrafluoroethylene (PTFE), called Teflon, against stainless steel. Sliding systems with a predefined coefficient of friction can provide seismic isolation by limiting accelerations and thus forces. Sliding systems are available in curved and flat surfaces. Curved sliding systems provide restoring forces because of their shape while flat sliders are required to be equipped with spring elements called Mass Energy Regulators (MER) to provide restoring forces. The MER elements reserve a part of the seismic energy to re-centre the bearing and structure after a seismic event. In addition, the MER system prevents excessive displacements of the structure. In this paper, test results of a sliding isolation system called “EradiQuake” (EQS) are presented. Figure 2 illustrates the components of a multidirectional EradiQuake isolator schematically.

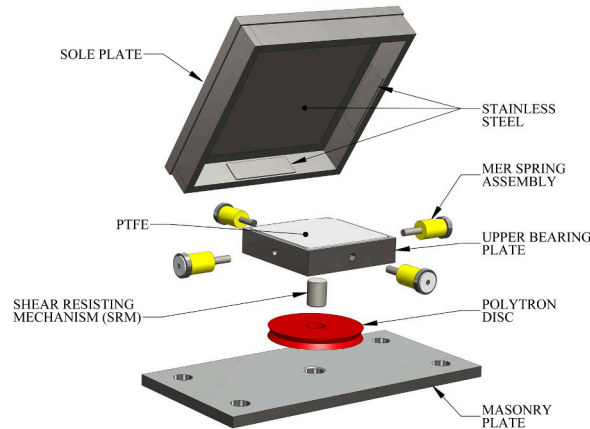


Figure 2. Components of a typical multidirectional EradiQuake seismic isolator.

TESTED ISOLATORS

The EradiQuake seismic isolation system was developed based on extensive research conducted at the National Center for Earthquake Engineering Research (NCEER) at the State University of New York at Buffalo [3]. Shake table testing confirmed that the EQS is an extremely effective system for significantly reducing forces and displacements caused by strong ground motion accelerations. A unique advantage of this seismic isolation system compared to others is that the flexibility of the isolator can be varied in different directions to reach the desired performance in the isolated structure under seismic excitations [4]. The sliding surface provides the required displacement capacity and dissipates the input energy through friction. Rotational capacity is provided through a polyurethane disc and a central pin transfers induced lateral forces from the superstructure to the substructure. Figure 3 shows dimensions of the tested EQS isolators. Two full-size prototypes were tested at École Polytechnique de Montréal and the in-house facility of the supplier during this project. Also, a part of testing program was conducted at the University of New York at Buffalo Structural Engineering and Earthquake Simulation Laboratory. According to the designer of the bridge, the seismic isolators are required to have the characteristics presented in Table 1 for normal temperature, 15 °C, and low temperature, -30 °C.

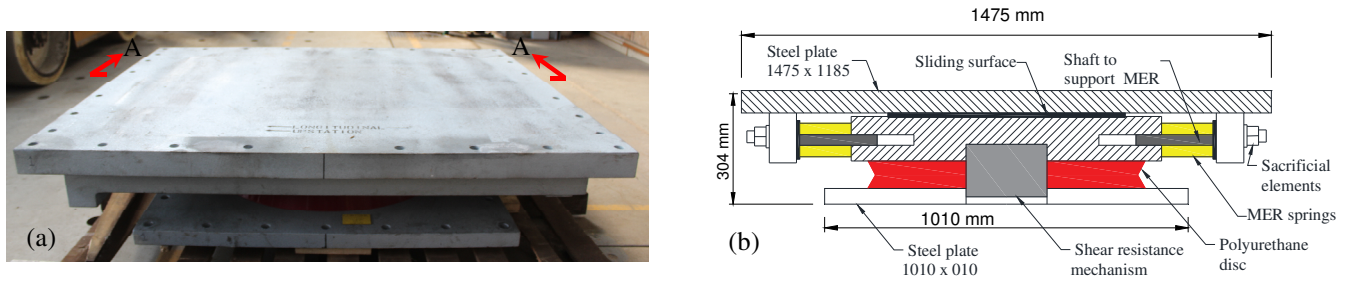


Figure 3. (a) A prototype, and (b) section A-A (no scale).

The bridge is isolated in the longitudinal direction and the seismic isolation system was designed to release when the forces exceed 850 kN per each isolator, thus, the isolators were equipped with a fuse system (sacrificial resistant system) in the longitudinal direction. The fuse system is designed to release over the given force and put the isolation system into action.

Table 1. Design characteristics of seismic isolators.

Test Temperature	combination	Q_d (kN)	K_d (kN/mm)	K_{eff} (kN/mm)	EDC (kN*mm)	F_y (kN)	β
+ 15 C	Average	760	5	20.8	145824	1000	0.48
	Peak of the first cycle	835	6.5	23.9	160406	1147	0.46
-30 C	Average	835	12.5	38.6	106938	1235	0.73
	Peak of the first cycle	919	16.3	45	117631	1439	0.41

TEST SET UP

Figure 4a shows a schematic elevation view of the test set-up used in these tests. The constant vertical force was provided by the 12 MN press. Horizontal displacements/forces were applied through a dynamic actuator with 1500 kN force capacity and stroke of ± 200 mm. The specimen was blocked in the set-up horizontally and a frictionless roller system was used between the press head and the sliding plate of the isolator. Figure 4b shows a photo of the set-up at École Polytechnique de Montréal.

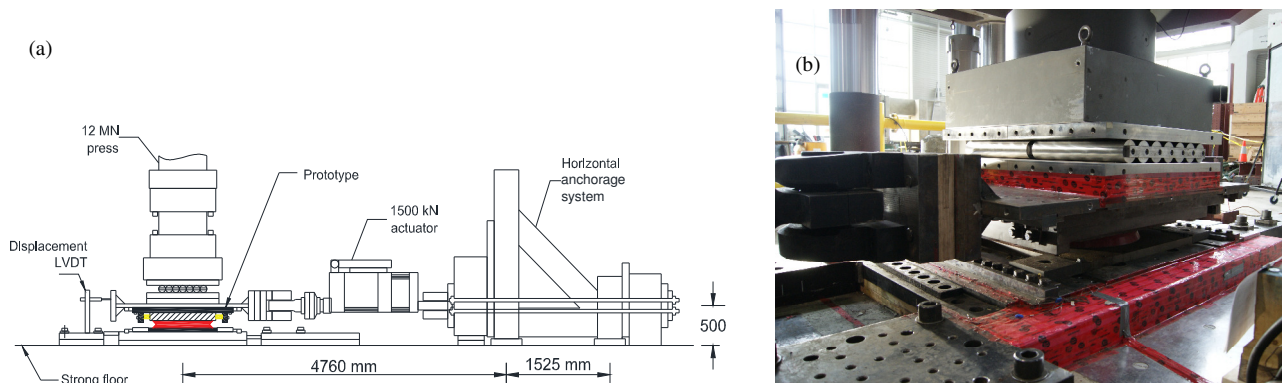


Figure 4. Polytechnique test set-up, (a) a schematic elevational view; and (b) a prototype isolator placed in the set-up.

TEST PROTOCOL

The test protocol included two types of loadings: i) non-seismic, and ii) and seismic. Each type of loading was applied in different sequences as presented in Table 2. The tests were mainly in accordance with CSA S6-06 [5]. It should be noted that in part b of the sequence 1, the 2014 edition of the CSA S6 [6] standard was used as this is a new requirement addressed in the 2014 edition of the standard. Also, the 2014 edition has stated clearly how to test the fuse system, therefore this edition was followed in testing the fuse system in part c of the sequence 1. The standard CSA S6-06 [5] has stated that the cold weather performance shall be considered in the design of seismic isolation systems in sustained low-temperature zones. This standard

does not present any tests concerning cold weather requirements. Therefore, the standard CSA S6-14 [6] was followed in cold temperature tests at sequence 7.

Table 2. Test protocol as per CSA S6 [5, 6] standard.

Sequence	Name	S6-06 clause	Number of cycles	Period (s)	Loading function	Vertical load (kN)	Horizontal displacement (mm)
0a	stability	4.10.11.2.(d)	1	100	sinus	13 563	$1.1\Delta_{max}$ (53)
0b	stability		1	100	sinus	9 223	$1.1\Delta_{max}$ (53)
1a	non-seismic	4.10.11.2.(c)	20	> 2	sinus	10850	
1b	non-seismic	4.10.9.2.3 S6-14		60		10850	
1c	restraint system			10850			
2	pause						
3a	seismic	4.10.11.2.(c)	3	1.56	sinus	10850	$0.25\Delta_{max}$ (12)
3b	seismic		3	1.56	sinus	10850	$0.5\Delta_{max}$ (24)
3c	seismic		3	1.56	sinus	10850	$0.75\Delta_{max}$ (36)
3d	seismic		3	1.56	sinus	10850	$1.0\Delta_{max}$ (48)
3e	seismic		3	1.56	sinus	10850	$1.25\Delta_{max}$ (60)
4	pause						
5	verification seismic	4.10.11.2.(c)	10	1.56	sinus		$1.0\Delta_{max}$ (48)
6	conditioning at -30 C for 48 hours						
7	low temperature seismic test	4.10.9.2.5.(b)	3	1.35	sinus	10850	$1.0\Delta_{max}$ (48)

TEST RESULTS

Sequence 0: stability tests

These tests were carried out as per CSA S6-06 [5] clause 4.10.11.2.(d). These tests were conducted at the 42 MN capacity in-house facility of the supplier because of the limit in the capacity of the vertical press at École Polytechnique. Two isolator bearings were placed back to back and tested simultaneously. Throughout investigations during and after the tests, no permanent deformations in the mating surfaces, cold flow in polyurethane discs, weld damages, or any other determinantal effects on the bearings were observed. Figures 5a and 5b show the hysteresis force-displacement behaviour of the two tested specimens.

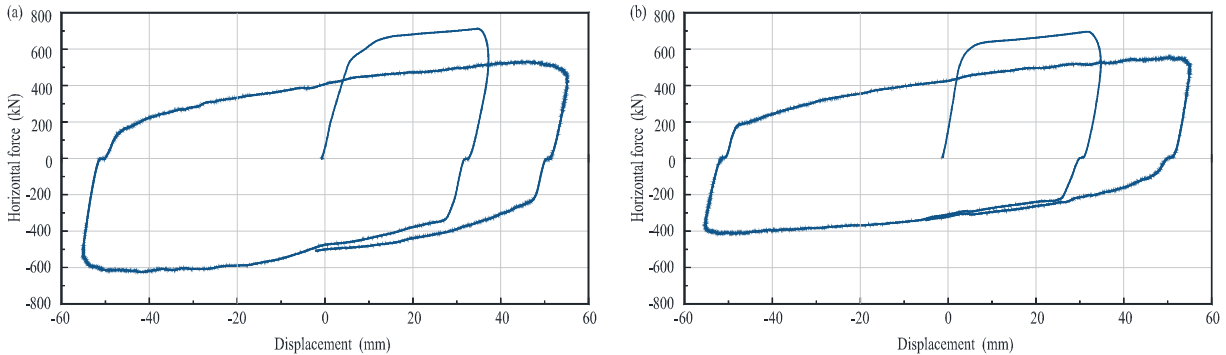


Figure 5. Force-displacement behaviour of the isolators in stability tests: (a) sequence 0a, (b) sequence 0b.

To determine the effective stiffness K_{eff} of the tested isolator in each displacement cycle, Eq. 1 was used [5, 6].

$$K_{eff} = \frac{F_p - F_n}{\Delta_p - \Delta_n} \quad (1)$$

where Δ_p and Δ_n are the maximum and minimum applied displacements, respectively. F_p is the horizontal force demand corresponding to the displacement Δ_p and F_n stands for the horizontal force demand corresponding to the minimum

displacement Δ_n . For the sake of clarity, the subscript "p" stands for positive (pushing) direction, and the subscript "n" denotes the negative (pulling) direction. The dissipated energy per cycle, EDC , is equal to the area under the hysteresis curve of the horizontal force-displacement in a given cycle that is obtained using a numerical integration. The equivalent viscous damping, β , in a given cycle can be obtained through the following equation [4, 5]:

$$\beta = \frac{EDC}{2\pi K_{eff} \left(\frac{\Delta_p - \Delta_n}{2}\right)^2} \quad (2)$$

Table 3 presents average characteristics of the EQS isolators during the stability test results. According to CSA S6-06 [5], all vertical load-carrying elements of the isolation system should remain stable under the specified displacements accompanied with the given level of vertical load. During these tests, each prototype remained stable showing a positive incremental force carrying capacity and no deterioration or damage were observed.

Table 3. EQS isolator characteristics in the stability tests.

Sequence	Max positive force (kN)	Max negative force (kN)	K_{eff} (kN/mm)	EDC (kN*mm)	Vertical load (kN)
0a	625.5	-530.5	10.51	99966	13563
0b	425.2	-320.8	6.78	88072	9223

Sequence 1: non-seismic tests

The sequence 1a was performed in accordance with Clause 4.10.11.2.(c).i of the CSA S6-06 [5]. Overall, 20 sinusoidal loading cycles with a horizontal force amplitude of 850 kN were applied on the prototypes in this step. The sequences 1b and 1c were conducted in agreement with Clause 4.10.9.2.3 of CSA S6-14 standard [6]. The sequence 1a started at centred position of the isolators and all cycles were applied at a frequency of 0.1 Hz. A vertical load of 10850 kN, equivalent to the gravity load of the bridge, was imposed before the beginning of the sequence and maintained until the end of sequence 1b. The sequence 1b included a quarter cycle of force control with a horizontal force amplitude of 850 kN, which was maintained for a period of 60 seconds. This sequence immediately started after the completion of sequence 1a so that the two sequences were performed continuously. Figures 6a and 6b show the hysteresis behaviour of the isolators. To determine the ultimate capacity of the sacrificial elastic restraint system, the sequence 1b was followed by a static monotonic test where the horizontal load was gradually increased up to failure of the elastic restraint system. According to the standard CSA S6-14 [6], the resistance of the sacrificial elements should be equal to or greater than 1.1 times the unweighted resistance of the system that is $1.1 \times 850 = 935$ kN. The measured resistance was 1173 kN and 1131 kN for prototypes 1 and 2, respectively. Both prototypes therefore comply with the requirement of standard CSA S6-14 [6] for the minimum resistance of the sacrificial restraint system as confirmed by the designer of the bridge.

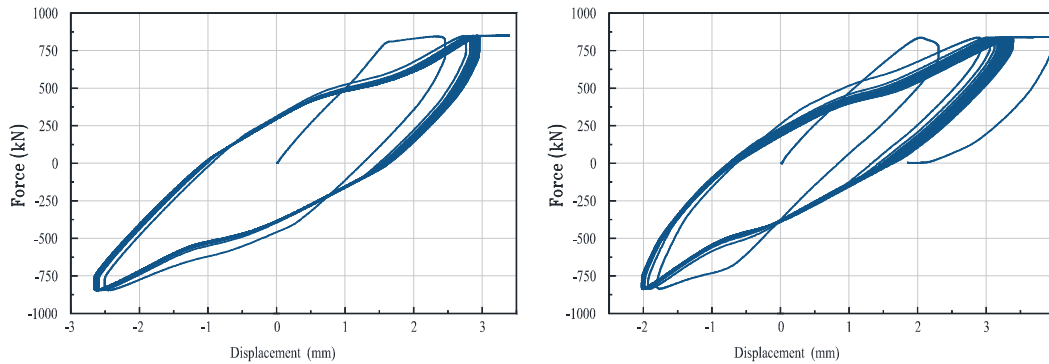


Figure 6. force-displacement behaviour of the isolators in non-seismic test. Left: prototype #1, Right: prototype #2.

Sequence 3: seismic tests

The sequence 3 was performed in accordance with CSA S6-06 Clause 4.10.11.2.(c).ii. It consisted of 5 sets of 3 sinusoidal displacement cycles at amplitudes equal to 0.25, 0.50, 0.75, 1.00, and 1.25 times the value of the total design displacement, 48 mm. The frequency was 0.64 Hz for all cycles. A constant vertical load equal to 10850 kN was imposed throughout the sequence. The behaviour of the prototypes is shown in Figure 7. The values of the effective stiffness, K_{eff} , dissipated energy per cycle, EDC , and the equivalent viscous damping, β , are presented for each of the test cycles of the sequence 3 in Table 4.

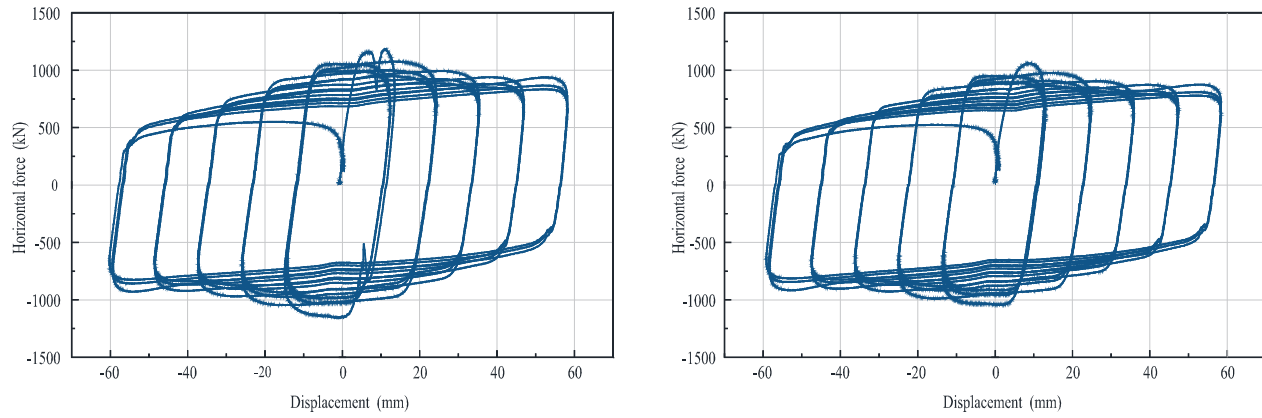


Figure 7. hysteresis behaviour of prototypes during sequence 3 of the test; LEFT: prototype #1, and RIGHT: prototype #2.

The average values of the effective stiffness, dissipated energy, and the equivalent viscous damping for each series of 3-cycles with the same displacement amplitude are also given in Table 4. The values of the ratio between the effective stiffness obtained of each cycle to the average effective rigidity for each series of 3-cycles are given in Table 4 as well. According to the results, due to the presence of the static friction at the beginning of the test, the first cycle with 12 mm amplitude shows relatively high rigidity compared to the following cycles.

Table 4. Seismic testing results, Left: prototype #1; and Right: prototype #2.

Ampl. (mm)	cycle	k_{eff} (kN/mm)	$\frac{k_{eff}}{k_{eff,av}}$	EDC	β	Ampl. (mm)	cycle	k_{eff} (kN/mm)	$\frac{k_{eff}}{k_{eff,ave}}$	EDC	β
12	1	103134	1.12	45.4	0.54	12	1	90728	1.09	41.1	0.54
	2	88500	0.96	43.4	0.56		2	80830	0.97	40.0	0.57
	3	85633	0.93	42.1	0.57		3	78662	0.94	38.9	0.57
	Ave.	92422		43.6	0.56		Ave.	83407		40.0	0.56
24	1	45534	1.06	89.6	0.58	24	1	41964	1.06	83.2	0.57
	2	42377	0.99	83.9	0.59		2	39051	0.99	77.5	0.58
	3	40415	0.95	80.8	0.58		3	37319	0.95	74.8	0.58
	Ave.	42742		84.7	0.58		Ave.	39445		78.5	0.58
36	1	28188	1.06	122.3	0.57	36	1	26231	1.05	113.6	0.56
	2	26293	0.99	115.1	0.57		2	24641	0.99	107.4	0.57
	3	25238	0.95	111.3	0.58		3	23798	0.96	104.1	0.57
	Ave.	26573		116.2	0.57		Ave.	24890		108.4	0.57
48	1	20117	1.05	148.1	0.55	48	1	19186	1.05	139.1	0.54
	2	18892	0.99	140.6	0.55		2	18038	0.99	133.0	0.55
	3	18229	0.96	136.2	0.55		3	17461	0.96	129.3	0.55
	Ave.	19079		141.6	0.55		Ave.	18228		133.8	0.54
60	1	16241	1.07	170.1	0.51	60	1	15576	1.07	161.5	0.50
	2	14969	0.99	161.7	0.52		2	14338	0.99	154.3	0.51
	3	14287	0.94	152.2	0.50		3	13692	0.94	145.6	0.50
	Ave.	15166		161.3	0.51		Ave.	14535		153.8	0.51

Concerning the system adequacy addressed in Clause 4.10.11.3.2 of the standard CSA S6-06 [5], for each increment of displacement in sequence 3, the variation between the effective rigidity of every cycle and the average effective rigidity of each series of 3-cycles should stay in the range of $\pm 10\%$. Also, more than 10% difference in the average value of effective stiffness of the two test specimens over the required three cycles of test is not allowed. According to the test results, both prototypes met these criteria for all cycles in the sequence except for the first cycle of the sequence 3a with 12 mm displacement for prototype 1. As is it obvious from Table 4, the ratio between the effective rigidity of the first cycle of sequence 3a to the average amount of the 3-cycle with 12 mm displacement is slightly higher and equal to 112%. Given that this value is close to the allowable limit of 110%, and that the situation occurred only for one cycle and for a single prototype, it can be concluded that the isolators have satisfied the intent of the criteria. Table 5 compares the effective rigidity and energy dissipation capacity of the two prototypes. According to Table 5, both prototypes met the requirements addressed in Clause 4.10.11.3.2.(b).ii. of the standard CSA S6-06 [5].

Table 5. Comparing rigidity and energy dissipation between two specimens.

Test sequence	Amplitude (mm)	Difference in $k_{eff,ave.}$ (%)	$\frac{EDC_{min}}{EDC_{max}}$	$\frac{EDC_{min}}{EDC_{max}}$
			prototype #1 (%)	prototype #2 (%)
3a	12	10.3	93	94
3b	24	8.0	90	90
3c	36	6.5	91	92
3d	48	4.6	92	93
3e	60	4.2	90	90

Sequence 5: verification seismic tests

The sequence 5 aims at investigating the conformity of the isolators with criteria addressed in Clause 4.10.11.3.2.(a) of the CSA S6-06 [5] standard. According to the mentioned Clause of the standard, it is required that the force-displacement curves show a positive incremental force-carrying capacity in all tests. Figure 8 presents the hysteresis behaviour of the prototypes under the loading of sequence 5. As it is obvious in Figure 8, the force-displacement curve obtained from the two prototypes has a negative incremental force in the first quarter of the first cycle. This negative incremental force is caused by a gradual transition from static to dynamic friction as well as the sinusoidal decreasing of actuator speed as it changes direction. The resistance of the prototypes tends to stabilize after the first cycle of the sequence. This change is attributed to a variation in the coefficient of friction at the PTFE-stainless steel interface as a function of the cumulative sliding distance. It should be noted that the actuation system has an important effect on the force response of the specimen in the beginning of the cyclic test. It is required to start the cycling with a very slow speed and increase the velocity to the target level instead of starting the test immediately with the maximum speed. Starting the test with the target velocity from the very early point of tests will cause a higher static friction and consequently a sharper negative incremental force in the first quarter cycle is created.

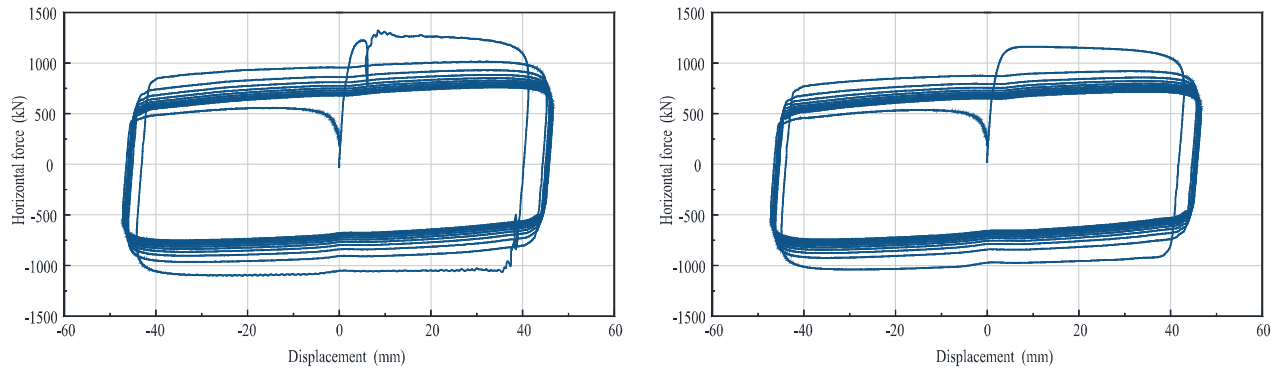


Figure 8. hysteresis behaviour of prototypes during sequence 5; LEFT: prototype #1, and RIGHT: prototype #2.

According to Clause 4.10.11.3.2.(c) of the CSA S6-06 [5], it is required that the increase or decrease in effective stiffness between the first cycle and all subsequent cycles be less than 20%. Also, Clause 4.10.11.3.2.(d) of the standard states that the reduction in the equivalent viscous damping over the duration of the test should be less than 20%. Both prototypes met these requirements.

Sequence 7: low temperature test

The sequence 7 of the test protocol was designed to simulate the loading addressed in Clause 4.10.9.2.5.(b) of the standard CSA S6-14 [6]. Due to limited capacity of the employed horizontal actuation system, it was decided to perform the low temperature test with 32 mm displacement and extrapolate the results for 48 mm. Prior to Seq. 7, the specimens were exposed to a temperature of $-30 \pm 5^\circ\text{C}$ for a period of 48 hours inside a closed chamber. After conditioning, three cycles with an amplitude of 32 mm at frequency of 0.74 Hz was applied. A constant axial load of 10850 kN was imposed during the sequence. In both prototypes, the target displacement could not be achieved in any of the 3 displacement cycles because the horizontal actuator reached its force capacity of 1500 kN after only 10 mm displacement in both directions. Both of the prototypes showed a very stiff behaviour that was initially rejected according to the target design values. To figure out the cause, both prototypes were disassembled, and every component was investigated. It was observed that due to many high-speed cyclic movements in previous steps, a PTFE layer had deposited onto the sliding stainless steel, so actually PTFE was sliding on PTFE which is known to be a higher friction condition. To adjust the sliding surface to meet project requirements, it was decided to do component testing (testing sliding surface and MER systems separately and then adding up the results) instead of doing full bearing assembly tests. Component testing was designed to reproduce results of the sequence 5, and to make sure that it can

show the behaviour of the full bearing assembly. After several trials, a semi-lubricated (33% lubricated and 67% dry) PTFE sliding surface was used to obtain the target results. Results of the semi-lubricated sliding interface showed a very good correlation between results of the sequence 5 and its equivalent component testing. The sliding surface and MER elements were conditioned in $-30\text{ }^{\circ}\text{C}$, 48 hours prior to low temperature testing sequence 7. It should be noted that in component testing a one-fourth scale of the sliding interface was tested and results were scaled up to full size for evaluation. In order to investigate the effect of displacement command signal, the component testing was performed using two signals: i) the initial signal that was used for fully assembly test in sequence 7 (rejected tests), and (ii) a modified signal starting with very slow speed and then increasing to the target velocity in a short period. Figures 9a and 9b show the results of component testing with modified and initial command signals, respectively. The effect of command signal on higher force demanding in the sliding surface during the first quarter cycle is evident. The results of component testing showed that the isolators comply with the requirements of CSA S6-14 [6] for low temperature. The component testing program was conducted at the University of New York at Buffalo.

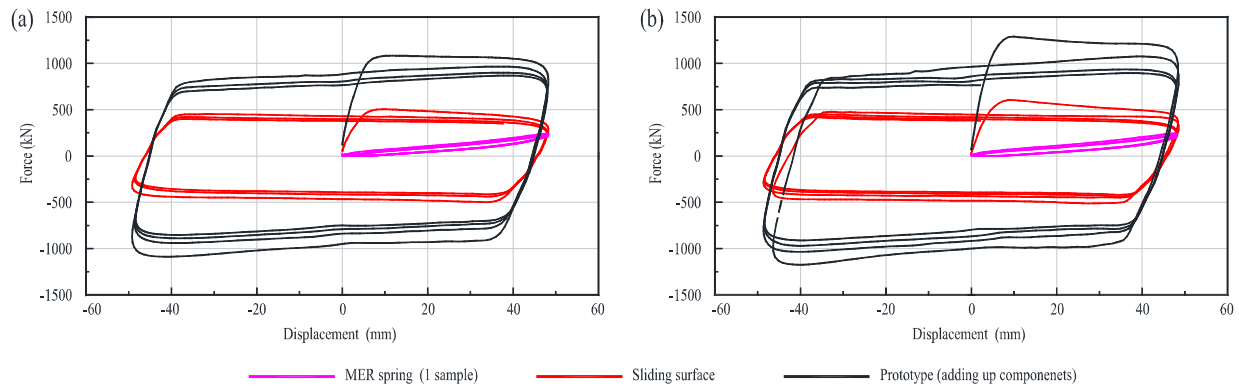


Figure 9. Components testing results: (a) Modified signal command., and (b) initial signal command.

After the qualification tests, the prototypes were refurbished by changing all non-metal parts and before installing on the bridge, quality tests addressed in AASHTO GSID [2] standard were performed. All tests were passed in accordance with the required criteria. Due to the limit in the number of pages of the paper, the detail results of the quality tests are not presented here.

CONCLUSION

Test results showed that friction-based EradiQuake systems can satisfy the testing requirements of current Canadian standards. It was very simple and quick to adjust the design requirements in the friction surface and simulate the required behaviour. In the case of cyclic testing of friction-based systems, the CSA S6 and AASHTO standards may recommend in future editions to change the sliding elements after a couple of cycles to prevent additional friction resulting from high speed wear of the PTFE or equivalent sliding material. It is highly recommended to start cycling very slowly in the pearly moments of the first cycle in order to avoid imposing unwanted impact type loadings. Starting cycling abruptly with the peak seismic speed, will increase the horizontal force response of the isolator unit and make it difficult to reveal the real characteristics of the friction-based isolation system under the design seismic tests. Providing a common signal command in the standards would also be useful.

ACKNOWLEDGMENTS

The authors gratefully acknowledge the help of Prof. Robert Tremblay and efforts of his laboratory team in the test program. Also, the authors wish to thank Justin Walker for his endeavours during the tests and Lucian S. Tataru for his help in drawings.

REFERENCES

- [1] Datta, T. K. (2010). *Seismic Analysis of Structures*. John Wiley & Sons (Asia) Pte Ltd, Clementi Loop, Singapore.
- [2] American Association of State Highway and Transportation Officials - AASHTO (2014). *Guide Specifications for Seismic Isolation Design, 4th edition*. Washington DC, USA.
- [3] Constantinou, M.C., Kartoum, A., Reinhorn, A.M., Bradford, P.F. (1991). *Experimental and theoretical Study of a Sliding Isolation System for Bridges*, Technical Report NCEER 91-0027, National State University of New York at Buffalo.
- [4] Gauron, O., Saidou, A., Busson, A, et Paultre, P. (2014). *Détermination des états limites des appuis et des isolateurs de ponts dans une approche basée sur la performance sismique*. Report No. MTQ-R716, Centre de Recherche en Génie Parasismique et en Dynamique des Structures, University of Sherbrooke, Sherbrooke, Canada.
- [5] Canadian Standard Association - CSA (2006). *CAN/CSA-A23.3: Design of concrete structures*. Toronto, ON.
- [6] Canadian Standard Association - CSA (2014). *CAN/CSA-A23.3: Design of concrete structures*. Toronto, ON.